Emission from weakly nonideal helium plasmas produced in flash lamps

Y. Vitel and M. El Bezzari
Laboratoire des Plasmas Denses, Université Pierre et Marie Curie, Tour 12 E5, 4 Place Jussieu, F-75252 Paris Cedex 05, France

L. G. D'yachkov and Yu. K. Kurilenkov
Institute for High Temperatures, Russian Academy of Sciences, Izhorskaya 13/19, Moscow 127412, Russia
(Received 11 February 1998; revised manuscript received 20 July 1998)

High pressure pulsed arcs produced in flash lamps filled with pure helium are applied for the generation of weakly nonideal plasmas characterized by a temperature $T\sim 2$ eV and a coupling parameter $\Gamma\sim 0.1$ (ratio of the mean electrostatic interaction energy of two charge carriers to their mean kinetic energy). Radiative emission from flash lamps in the spectral range 300–850 nm is measured and calculated, taking into account the nonideal effects (through plasma quasistatic microfields) and the inhomogeneity of the arc plasma. Radial profiles of temperature and particle densities are deduced from the measurements of neutral line intensities and transverse distributions of emission. Temperature and electron density values are also obtained from absorption and laser interferometric measurements, respectively. Calculated and measured plasma spectra obtained are in good agreement at electron densities $\sim 10^{18}$ cm^{-3}. [S1063-651X(98)13212-9]

PACS number(s): 52.25.Qt, 52.70.Kz

I. INTRODUCTION

The problems of dense plasma emission, opacity, radiative transfer, and energy transport under moderate and strong coupling are of both fundamental and applied interest [1,2]. The density effects in plasma radiation were the subject of a considerable number of experimental and theoretical studies in the last few decades; however, our understanding and knowledge are still incomplete even for moderately dense plasmas. The level and character of manifestation of plasma density effects are different in dilute, moderately dense, and extremely dense (strongly coupled or nonideal) plasmas. Thus different models have to be applied for description of plasma radiation spectra: conceptions of isolated atom, weakly perturbed, or strongly perturbed ones should be used correspondingly.

Atomic physics concepts dominate in the opacity problem when emission or absorption of dilute plasmas is considered [3,4], but under extreme plasma densities the coupling effects and correlations may be very important for description of optical properties (e.g., [5,6]). In the low and moderately dense plasma spectra the principal density effect is the transformation of the spectral line series in the near-threshold region to a continuum due to the line overlapping and merging. In the hydrogenic plasma, if only upper members of the line series are perturbed, this case corresponds to the well-known Inglis-Teller model for apparent shift of photorecombination (photoionization) thresholds. Note that description of the near-threshold spectra based on the line broadening and merging is not so simple due to a lot of lines and some computation problems. Usually this approach needs a certain ''*ad hoc*'' operation [7,8]. A more adequate approach is based on the microfield model, which has been derived by many authors [8–17]. It assumes that when the plasma microfield is strong enough, the higher excited atomic levels disappear while continuum states appear. Thus, in the near-threshold region, not only the merging of lines (quasicontinuum) is supposed, but also the decrease of their intensities and substitution by a photorecombination continuum (real continuum). This calculation scheme suggests two physically clear assumptions: first, statistical character of quasistatic microfield action on atoms and ions in a plasma and, second, undisturbed density of oscillator strengths for radiators ''perturbed'' by surrounding plasma. A rather wide range of the plasma parameters is available which corresponds to this approximation. Under strong coupling, the redistribution of dense plasma absorption along the spectrum, and related ''transparency windows'' before the series limits, are the subject of studies and discussions [5,14,18]. A good agreement of calculations based on this theoretical scheme with experimental data for continuous radiation of moderately dense noble gas plasmas (neon, argon, krypton, and xenon at electron densities up to 10^{18} cm^{-3}) was found [19]. Continuous radiation of helium plasmas has not been previously measured quantitatively for such electron densities, to our knowledge. Note that reliable dense plasma diagnostics based on radiation continuum and spectral line intensities have to take properly into account the density and coupling effects.

Most of the experimental investigations on dense cold helium plasmas in recent years have been devoted to neutral line Stark broadening and shift studies [20–22]. However, the total emitted radiation spectra (relations between continuum and spectral lines) have not been studied in detail. Our aim in this work is to remedy experimentally this defect and to give a theoretical description of the helium radiation spectrum taking into account the influence of the plasma environment on radiators. Helium plasma has several advantages for the detailed study of the plasma density effects in radiation, for example, due to spectral simplicity (in comparison with plasmas of complex elements) and absence of the linear Stark effect (as for the hydrogen atom).

Helium high pressure arcs created in this work in linear flash lamps have a good cylindrical symmetry, are very reproducible, and are in local thermodynamic equilibrium. On axis electron densities of around 10^{18} cm^{-3} and temperatures

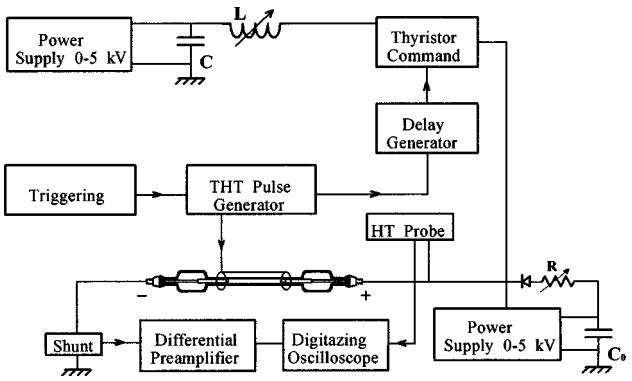

FIG. 1. Diagram of the electrical experimental setup.

in the range $(2-3)\times10^4$ K are achieved. In these conditions, the mean interaction potential energy between charged particles E_p is appreciable compared to their kinetic energy E_k. The coupling parameter $\Gamma=E_p/E_k$ is in the range 0.1–0.2. The number of particles in the Debye sphere is small and around unity. Thus we are dealing with weakly nonideal but formally, non-Debye plasmas. In fact, flash lamps provide a very convenient and efficient tool to study consequently the density and coupling effects in moderately dense plasma spectra and clarify the possible tendencies for density effects in opacities [23,24]. This problem is especially delicate for the plasmas with moderate densities, where the possible deviations from ideal plasma theory results are comparable with the accuracy of the measurements themselves. On the other hand, these effects will be very important for adequate description of radiative opacities and energy transport in extremely dense laboratory and astrophysical helium plasmas, and have to be studied consequently at the different stages as plasma density grows.

We present in the following the results of different optical and electrical measurements in dense helium plasmas. We describe the experimental setup (Sec. II), the methods of calculations (Sec. III), and diagnostics (Sec. IV) used to determine the plasma parameters, present obtained radial profiles of temperature and electron and atomic densities, and compare measured and calculated spectra (Sec. V). Then, the place of the results obtained among other noble gas plasma data is discussed briefly (Sec. VI).

II. EXPERIMENTAL SETUP

The plasmas are produced in fused quartz linear flash lamps whose inner diameter is 5 mm and distance between electrodes is 100 mm. These lamps are filled with pure helium at initial pressures from 50 to 500 Torr. Special ballast volumes behind the electrodes are disposed to reduce losses of helium pressure due to particle diffusion through the wall. In Fig. 1 a schematic view of the electrical experimental setup is displayed. The gas breakdown is performed applying a high voltage pulse (30 kV, 1 μs) on an external auxiliary electrode. Then, a low current ($\approx$1 A) simmer is maintained during 12 ms before triggering the main discharge to ensure the discharge centering on tube axis. By this method, the plasma-wall perturbative phenomena are minimized, as described by Vitel *et al.* [25] and by Vitel and Skowronek [26]. The electrical pulse is produced by means of an *LC* cell with variable inductance, which permits us to adapt the source impedance to the plasma impedance. The maximum current intensity is set in the range 0.5–1.6 kA and its pulse duration at half maximum is around 100 μs. The voltage drop across the tube is measured by a precise ($\pm1\%$) voltage divider, and the current intensity by a coaxial shunt ($R=0.25$ mΩ $\pm0.2\%$) connected to a differential amplifier. Both signals are recorded on a digital oscilloscope and processed by a personal computer.

The experimental setup used for optical measurements is shown in Fig. 2. Two spectrographs with different dispersions, coupled with a gated intensified charge coupled device (ICCD) or photodiode array (OMA), are used to measure and record the spectra. All spectral measurements are performed during a short period of time (less than 1 μs) at the current maximum, when the best filling of the plasma is obtained inside the flash lamp. For standardization purposes, we use a calibrated deuterium lamp for wavelengths below 350 nm and a tungsten ribbon lamp for the spectral range 350–900 nm. The wavelength scale is calibrated using spectral lamps.

III. METHOD OF CALCULATION

Radiation spectrum of helium plasma in the conditions considered is formed from bound-bound (spectral lines), free-bound (radiative recombination), and free-free (brems-

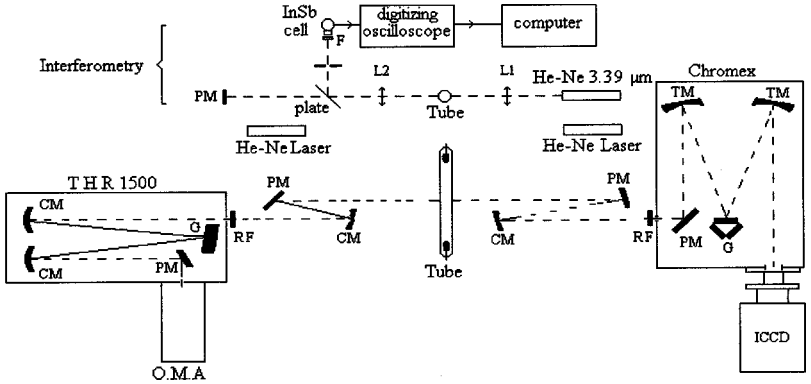

FIG. 2. Scheme of the optical experimental setup: OMA, optical multichannel analyzer (intensified photodiode array detector, 1024 pixels); ICCD, intensified charge coupled device (584×384 pixels); THR 1500, spectrograph ($f=1500$ mm, grating 1800 g/mm); Chromex spectrograph ($f=250$ mm, three gratings 600, 1200, and 2400 g/mm); RF, high order rejecting filter; PM, plan mirror; CM, concave mirror; $L1$ and $L2$, infrared lenses ($f=200$ mm), He-Ne laser (632.8 nm) for optical alignment.

strahlung) transitions. The line profiles are not studied in detail in this paper. The line broadening and shift parameters are calculated according to Griem [27], while the line intensities are estimated taking into account their decrease (so-called line dissolution) due to disappearance of the radiating levels E under the influence of the quasistatic plasma microfields [8–17]. For the electron on an atomic level a potential barrier is formed in the direction of the quasistatic ion microfield. If the microfield is strong enough, more than a certain critical value $F_c(E)$, the discrete level is turned out above the barrier and disappears. The probability of the level realization is then defined as the integral of the microfield distribution function

$$W(E)=\int_0^{F_c(E)} P(F)dF. \tag{1}$$

We use the quasistatic distribution function of Hooper [28] for a neutral point (where a neutral atom is placed) and express integral (1) with the analytical approximation derived by D'yachkov [29]. For the determination of the critical value F_c, we use two simple models, uniform field (UF) and nearest neighbor (NN) approximations. These approximations give different values of the critical field: $F_c(E)=E^2/4e^3$ (UF) and $F_c(E)=E^2/16e^3$ (NN) for a state with ionization energy E in an unperturbed atom [15,17]. For one-electron atoms UF is reasonable [17,30], while for many-electron atoms NN is more appropriate [16,19]. It should be noted that for a broadened level, one can calculate from Eq. (1) the realization probability for each value of E within the level width ΔE. So, the variation of $W(E)$ on ΔE leads to a slight deformation of the corresponding line profile.

The photorecombination and bremsstrahlung transition rates are calculated using the semiclassical approximation within the framework of the quantum defect theory [19,31–33]. Assuming that the spectral density of oscillator strengths [34] in the near-threshold region is conserved [35,36,5], we continue the radiative recombination continuum multiplied by the factor $1-W$ over its long-wavelength threshold in order to compensate for the decrease of the line intensities. Near the threshold $W\to 0$, while $W\to 1$ away from threshold. Therefore the line series transform gradually to a continuum. The method of calculation is given in detail by D'yachkov [33] and D'yachkov, Kurilenkov, and Vitel [19]. In contrast to the method of Hofsaess [37], it takes into account smoothing effect on the photorecombination thresholds when the plasma density increases due to the quasistatic ion microfield. The free-bound ξ function allowing for the specific features of a nonhydrogenic atom [35,37] is shown in Fig. 3 for a few values of the electron density (it is similar to the average Gaunt factor, since it also gives the ratio of the quantity under consideration to the corresponding hydrogenic one in the Kramers approximation). The UF and NN approximations are used for estimations of the critical values of the microfield. In the case of ideal plasma ($N_e\to 0$) our calculation is in a good agreement with that of Hofsaess [37] (in Ref. [37] splitting of the $2^{1,3}P$ threshold near 350 nm is not taken into account). However, the ξ function for a dense plasma may differ considerably from that of the ideal plasma and, furthermore, the functions corresponding to the UF and NN models differ significantly from each other. The difference between UF and NN models corresponds approximately to one order of magnitude in electron density.

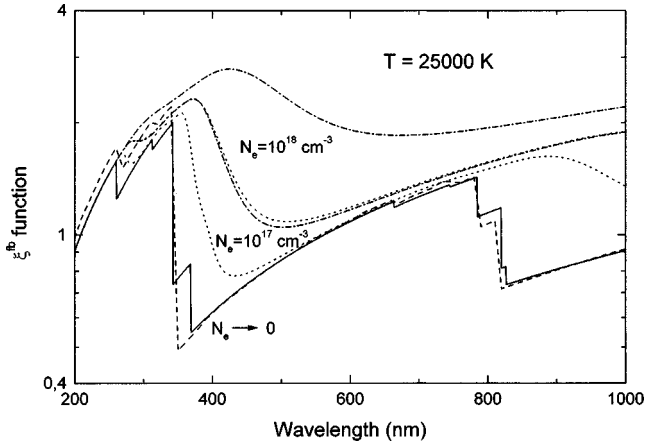

FIG. 3. Free-bound ξ function of helium for $T=25\,000$ K. Comparison of our calculation for ideal plasma ($N_e\to 0$, solid curve) with that of Hofsaess [37] (dashed curve). For dense plasmas ($N_e=10^{17}$ and 10^{18} cm^{-3}) both UF (dotted curves) and NN (dashed-dotted curves) models are used for the estimation of critical values of the microfield.

Since the helium plasma in the discharge tube is inhomogeneous, the radiation intensity from the flash lamps is calculated taking into account radial profiles of temperature and electron and atom densities. The method to determine the profiles is given in Sec. IV A.

The plasma in the conditions under consideration is optically thin except the line at 587.5 nm, for which the optical thickness $\tau\sim 1$. Therefore we should take into account the self-absorption, however, we can restrict ourself to the one-dimensional approximation. Then the equation of radiative transfer along an x axis has the form

$$\frac{dJ(\lambda,x)}{dx}=\varepsilon(\lambda,x)-k'(\lambda,x)J(\lambda,x), \tag{2}$$

where $\varepsilon(\lambda,x)$ and $k'(\lambda,x)$ are the emission and absorption coefficients, respectively; the last takes into account the induced emission, $k'(\lambda,x)=k(\lambda,x)[1-\exp(-hc/\lambda kT)]$. These coefficients depend on x as a function of local values of the temperature and electron density

$$\varepsilon(\lambda,x)\equiv\varepsilon(\lambda,T(x),N_e(x)),\quad k'(\lambda,x)\equiv k'(\lambda,T(x),N_e(x)).$$

Under the condition of local thermodynamic equilibrium (LTE) they are related to each other by the Kirchhoff law

$$\varepsilon(\lambda,x)=k'(\lambda,x)B(\lambda,T(x)), \tag{3}$$

$$B(\lambda,T)=2hc^2\lambda^{-5}(e^{hc/\lambda kT}-1)^{-1}. \tag{4}$$

The solution of Eq. (2) is

$$J(x)=\exp\left[-\int_0^x k'(x')dx'\right]\times\left\{J_0+\int_0^x\varepsilon(x')\exp\left[\int_0^{x'}k'(x'')dx''\right]dx'\right\}$$

(here and below the variable λ is omitted, if it is not necessary), where J_0 is the integration constant $J_0=J(0)$. In the case of axial symmetry and boundary condition $J_0=J(-R)$, for the emission along the diameter of the tube $[\varepsilon(-r)=\varepsilon(r)]$ we have

$$J(R)=J_0e^{-\tau}+2e^{-\tau/2}\int_0^R \varepsilon(r)\cosh[t(r)]dr, \qquad (5)$$

where R is the radius of the flash lamp,

$$t(r)=\int_0^r k'(x)dx,$$

and $\tau=2t(R)$ is the optical thickness of the discharge plasma. $J_0=0$ if only the flash lamp is an emission source.

IV. DIAGNOSTICS

For the calculation of the radiation intensity of helium plasma in flash lamps, the radial profiles of temperature $T(r)$ and electron $N_e(r)$ and atom $N_a(r)$ densities are required. Since direct measurements of the profiles are impossible, their determination is based on the comparison of the spectral measurement data with calculations. However, in this case an additional verification independent of theory is desirable. The electron density is verified by the He-Ne infrared laser interferometry at 3.39 μm. Independent determination of temperature can be carried out from measurements of the optical thickness.

A. Radial profiles of particles and temperature

The transverse distribution of the emitted light radiation is recorded in narrow spectral ranges (0.4 nm) free of perturbing lines where the plasma is optically thin (around 780 and 820 nm). All the measurements are taken at the current maximum (during 1 μs with a spatial resolution of 50 μm). Applying the well-known method of the Abel integral, radial dependence of the emission coefficient $\varepsilon(r)$ is deduced. This coefficient is related to the plasma parameters by the formula

$$\varepsilon(\lambda,r)=\frac{8}{3}\left(\frac{2\pi}{3}\right)^{1/2}\frac{e^2}{c^2m^{3/2}}\frac{N_e^2(r)}{\lambda^2\sqrt{kT(r)}}\,\xi(\lambda,T(r),N_e(r)), \qquad (6)$$

where the ξ function, in the general case, includes free-free, free-bound, and bound-bound transitions (although the contribution of line wings is small and constitutes here a few percent, it is taken into account in calculations).

A computing iterative procedure is applied to obtain the particle densities and temperature profiles. First, an initial temperature on axis $T(0)$ is given and from Eq. (6) with the experimental value $\varepsilon(0)$ and ξ function, calculated according to Refs. [19,27], we get $N_e(0)$ and, using the Saha equation and the Dalton law, find the atom density $N_a(0)$ and pressure $p(0)$. In the Saha equation and the Dalton law the corrections from the nonideality are introduced [38]. Then, on the basis of constant pressure in the quasistationary phase of the plasma column around the maximum of the current, using the same equations, we deduced from each value of $\varepsilon(r)$ the corresponding values of $T(r)$, $N_e(r)$, and $N_a(r)$. As a result, we have the radial profiles corresponding to the initial value $T(0)$ and experimental profile $\varepsilon(\lambda,r)$ at fixed λ. Next, with those evaluated profiles the neutral line intensity integrated along a diameter (at 587.5, 667.8, or 706.5 nm) is calculated and compared to the experimental one. If both values are not in agreement, the initial axis temperature $T(0)$ is modified and the entire procedure is repeated until the calculated and experimental values of the line intensity agree within 1%.

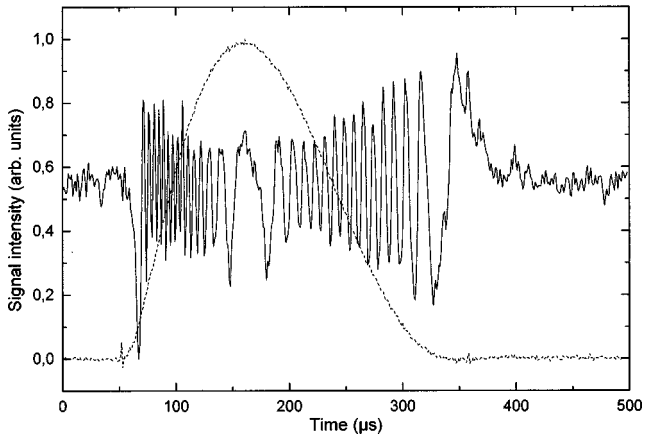

FIG. 4. Interferogram (solid curve) and current pulse profile (dashed curve) for discharge at initial pressure 400 Torr and $I_{max}=1130$ A.

In the calculation the total LTE is assumed. Possibility of its violation is analyzed in Sec. V A.

In the calculation the separation of the line from the continuum background is carried out in the same manner as in experiment. Using the trial profiles corresponding to given $T(0)$, we calculate the radiation intensity spectrum in the range near the line and extract its contribution by analogy with experimental procedure. This is important, since in the measured spectrum at high temperature and electron density, the separation of the wings from the continuum is a difficult problem.

B. Optical thickness and average temperature

The confirmation of the values of temperature found by the method of Sec. IV A is given from the temperature estimation obtained from absorption measurements of the He I line at 587.5 nm for which $\tau\approx1$. Its opacity is determined by means of a concave mirror set behind the flash lamp on the optical axis and reflecting back the plasma radiation with a magnification of one through itself. From the recorded spectra taken with and without the concave mirror, the line optical thickness is deduced. In the case of the spectrum recorded with the mirror we should set in Eq. (5) $J_0=KJ_1$ where J_1 is the spectral emission intensity without the mirror expressed by the second term in Eq. (5) and K is the coefficient allowing for reflectivity of the mirror and tube wall. Thus the total intensity with the mirror is

$$J_2(\lambda)=J_1(\lambda)(1+Ke^{-\tau(\lambda)}).$$

Consequently, carrying out the spectral measurements with and without the mirror, we can get the optical thickness as a function of wavelength.

TABLE I. On axis temperatures and electron densities obtained, using classical calculation, from the radial dependence of the emission coefficient at $\lambda = 780$ nm and the intensity of the spectral line at 587.5 nm for a flash lamp at an initial pressure of 400 Torr.

I_{max} (A)	$T(0)$ (K)	$N_e(0)$ (cm^{-3})
715	33 000	9.95×10^{17}
850	36 100	1.12×10^{18}
1000	39 800	1.27×10^{18}
1130	41 400	1.47×10^{18}
1280	42 800	1.58×10^{18}

In the approximation of homogeneous plasma, we have from Eq. (5) that

$$J_1(\lambda) = B(\lambda, T)(1 - e^{-\tau(\lambda)}), \tag{7}$$

where $B(\lambda, T)$ is the Planck function [Eq. (4)]. Solving Eq. (7) for T, we can obtain a certain average temperature from the experimental values of $J_1(\lambda)$ and $\tau(\lambda)$ as a function of λ. Usually the Bartels method [39,40] is applied to take into account the weak radial inhomogeneity of the plasma and to find the temperature on axis, however, we evaluate the opacity in the calculation and, thus, this method is not needed.

C. Interferometric measurements of electron density

To check the values found for the electron density profiles, we have used an Ashby-Jephcott interferometer [41,42] at the wavelength of 3.39 μm (He-Ne laser) where the refractive index of the plasma is due only to the electron density. Figure 4 shows an example of a recorded interferogram due to the refractive index evolution along a diameter during the discharge. Taking the relative shape of the electron density profiles previously determined, we calculated their absolute values leading to the number of modulations measured on the interferograms.

V. RESULTS

A. Plasma parameters

The plasma parameters deduced from continuum and line intensities (at 587.5, 667.8, and 706.5 nm) on the basis of classical plasma calculations are in disagreement with those deduced from opacity measurements (for T) and interferometry (for N_e). In Table I are presented $T(0)$ and $N_e(0)$ values so calculated for 587.5 nm He I line intensities and continuum at 780 nm in the case of a flash lamp filled at 400 Torr of initial pressure. $T(0)$ values are by far too high and would have to lead to observation of ionic helium lines on spectra but we have never seen one. Identical anomalous results were obtained with the other two lines which are practically optically thin.

But, if we take into account the effect of the statistical ionic microfields on the atomic levels in the calculation of the continuum and the line intensities, an agreement is obtained in the evaluation of the plasma parameters by those different methods and the evolution of $T(0)$ versus the initial pressure is correct. We report in Table II the temperature and electron density on the axis obtained for different discharge conditions in the case of a flash lamp filled at 400 Torr of initial pressure. Optical measurements are performed at $\lambda = 780$ nm (transverse distributions of emission) and in the range 556–620 nm (intensity of the 587.5 nm line). To determine the critical values of the quasistatic ion microfield both UF and NN approximation have been applied. In the last column the data of interferometric measurements of electron density with the He-Ne laser (3.39 μm) are given. They agree best with results obtained from the UF approximation.

In the case of the NN approximation the temperatures $T(0)$ are lower than for the UF approximation for the two first conditions in Table II, but for the other conditions no solution exists in the NN approximation. In this case the line dissolution is more pronounced. On the other hand, it is known that the relative contribution of the lines to the spectral intensity increases as the temperature decreases. So, the temperature is lower in the NN model in order to compensate for the line dissolution. However, according to Eq. (3), the absorption coefficient increases as the temperature decreases if the emission coefficient is fixed; consequently, the atom density and optical thickness in the line increase too. Thus the line intensity may be bounded because of self-absorption. So for three conditions with higher current, in the NN approximation the intensity of the 587.5 nm line is lower than in experiment for any values $T(0)$. For lower currents solutions exist, however, the corresponding atomic densities are too high, higher than initial density at 400 Torr and T

TABLE II. Temperature and electron density on axis at an initial pressure of 400 Torr, obtained from the radial dependence of the emission coefficient at $\lambda = 780$ nm and the intensity of the spectral lines at 587.5 nm, using the UF and NN approximations for the determination of the critical values of the microfield. Values in parentheses correspond to atomic densities higher than the initial one and, consequently, are incorrect.

		Optical measurements				
		UF		NN		Interferometric measurements
U (V)	I_{max} (A)	$T(0)$ (K)	$N_e(0)$ (cm^{-3})	$T(0)$ (K)	$N_e(0)$ (cm^{-3})	$N_e(0)$ (cm^{-3})
800	715	27 200	9.42×10^{17}	(19 700)	(7.99×10^{17})	8.69×10^{17}
900	850	28 200	1.06×10^{18}	(18 900)	(8.70×10^{17})	1.00×10^{18}
1000	1000	28 200	1.18×10^{18}			1.07×10^{18}
1100	1130	28 400	1.35×10^{18}			1.28×10^{18}
1200	1280	28 800	1.45×10^{18}			1.31×10^{18}

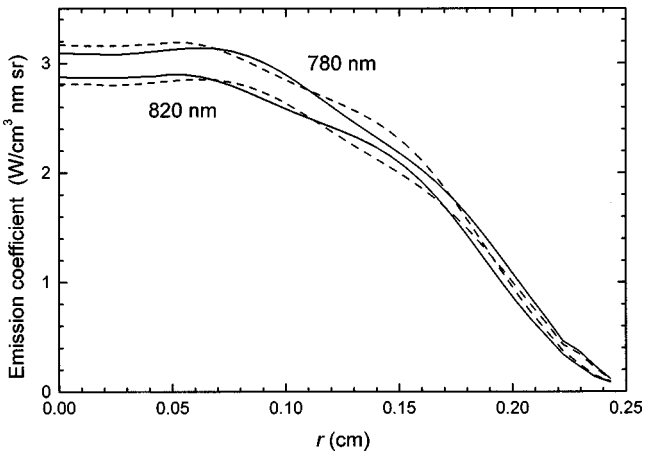

FIG. 5. Radial dependence of the emission coefficient in flash lamps at initial pressure 400 Torr and voltage 1000 V for $\lambda = 780$ and 820 nm. Experimental data are presented by solid curves. Dashed curves show the calculations of $\varepsilon(\lambda,r)$ with the temperature and particle profiles (Fig. 6) obtained from other λ [profiles from 820 nm for $\varepsilon(780,r)$ and profiles from 780 nm for $\varepsilon(820,r)$]. Calculations of $\varepsilon(\lambda,r)$ with profiles obtained from the same λ coincide with experimental curves.

$=300$ K which is 1.32×10^{19} cm^{-3}; in such a case the values in Table II are given in parentheses; obviously, they are unreliable.

More detailed spectral measurements are performed at initial pressure 400 Torr and $U=1000$ V ($T_{\max}=1000$ A). Radial functions of the emission coefficient $\varepsilon(\lambda,r)$ obtained from the transverse distributions of the radiative intensity measured at $\lambda=780$ and 820 nm are presented in Fig. 5 by solid curves. In Table III the values of the temperature on axis defined from $\varepsilon(\lambda,r)$ for $\lambda=780$ nm and intensities of neutral helium lines at 587.5, 667.8, and 706.5 nm are shown. For the 587.5 and 706.5 nm lines the data from two measurement runs are presented. For the lines at 667.7 and 706.5 nm solutions in the NN approximation exist, however, they may be false (values in parentheses), since the corresponding particle densities are higher than the initial one. For $\varepsilon(\lambda,r)$ at $\lambda=820$ nm results are approximately the same as those for $\varepsilon(\lambda,r)$ at 780 nm, the difference between corresponding values $T(0)$ is less than 100 K.

As a result, we can conclude that for the helium atom the UF model is as successful as in the case of hydrogen [17,30],

TABLE III. Temperature on axis at initial pressure of 400 Torr and $I_{\max}=1000$ A, obtained from the radial dependence of the emission coefficient at $\lambda=780$ nm and the intensity of different spectral lines, using UF and NN approximations for the determination of the critical values of the microfield. Values of $T(0)$ in parentheses correspond to particle densities higher than the initial one and, consequently, are incorrect.

	$T(0)$ (K)	
Line (nm)	UF	NN
587.5	28 200, 25 100	
667.7	23 900	(18 500)
706.5	26 000, 25 000	22 700, (21 900)

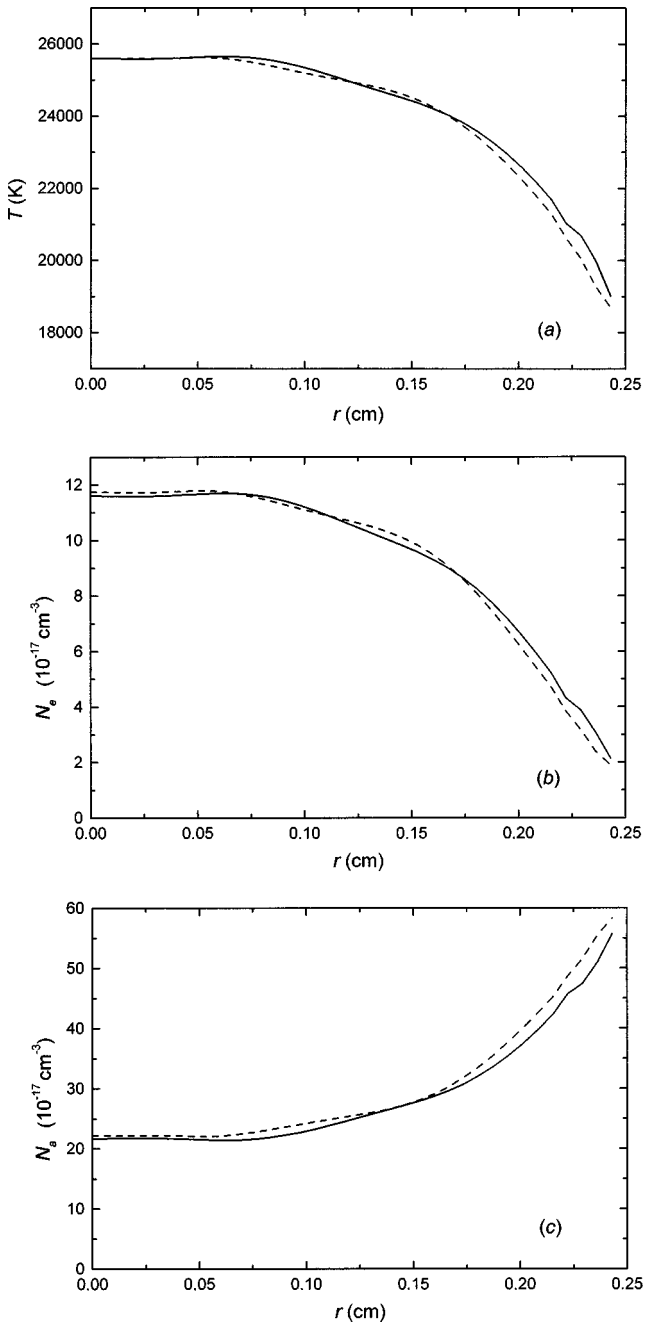

FIG. 6. Radial profiles of temperature (a), electron (b), and atomic (c) densities defined from the experimental profiles of the emission coefficient (Fig. 5) at $\lambda=780$ nm (solid curves) and 820 nm (dashed curves) for a discharge at initial pressure 400 Torr and voltage 1000 V.

while the NN model is incorrect in contrast to the case of heavy noble gas atoms [16,19].

For the following spectral calculations we set $T(0)$ equal to the mean over the values in Table III for the UF approximation. The error may be evaluated as the root-mean-square deviation. Thus we have $T(0)=25\,600\pm1500$ K. Corresponding particle and temperature profiles obtained from $\varepsilon(\lambda,r)$ at $\lambda=780$ and 820 nm are presented in Fig. 6. It is seen that profiles from $\lambda=780$ and 820 nm are close to each other. Calculation of $\varepsilon(\lambda,r)$ with profiles obtained under the same λ [$\varepsilon(780,r)$ with profiles from $\lambda=780$ nm and $\varepsilon(820,r)$ with profiles from $\lambda=820$ nm] coincide with cor-

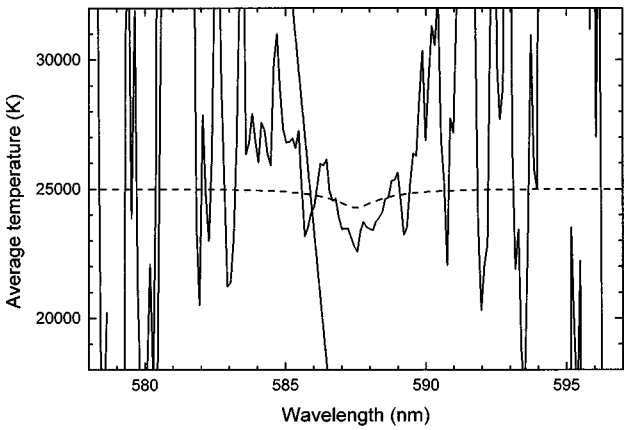

FIG. 7. Average temperature defined in the approximation of the homogeneous plasma [Eq. (7)] for the spectral region near the 587.5 nm line for a discharge at initial pressure 400 Torr and voltage 1000 V. Solid curve, experiment; dashed curve, calculation. In the line wings where $\tau \ll 1$, experimental definition of temperature is impossible due to the scatter in the data on $\exp(-\tau)$.

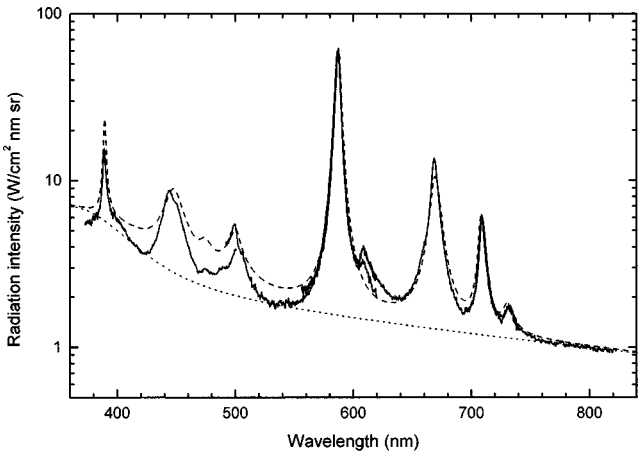

FIG. 8. Spectral emission from flash lamps filled with helium at initial pressure 400 Torr and voltage 1000 V. Solid curves, experiment; dotted curve, calculation, contribution of continuum; dashed curve, calculation, continuum and spectral lines.

responding experimental data in Fig. 5 (solid curves), which confirms the accuracy of the calculation. The emission coefficients $\varepsilon(\lambda,r)$ calculated with other profiles [$\varepsilon(780,r)$ with profiles from $\lambda = 820$ nm and $\varepsilon(820,r)$ with profiles from $\lambda = 780$ nm] are shown in Fig. 5 by dashed curves. In the spectral calculations we use the profiles corresponding to $\lambda = 780$ nm. In the calculation of the profiles, the total LTE has been assumed. However, violation in the near-wall region would be expected. The principal reason for departures from LTE in this region is the diffusion of atoms in the ground state. The criterion of the LTE existence in this case is that the variation of the plasma temperature ΔT on the diffusion length d has to be small [43,44]. Near the flash lamp wall $d \approx 0.03$ cm and $\Delta T(d) \approx 2000$ K. The near-wall region gives a small contribution to the flash lamp emission and such a failure of LTE cannot lead to significant influence on the result obtained.

The average values of temperature defined from the optical thickness $\tau(\lambda)$ in the homogeneity approximation according to Eq. (7) are given in Fig. 7. It should be noted that this quantity can be well defined from Eq. (7) if τ at least is of the order of unity (not less), which is the case only for the 587.5 nm line. If $\tau \ll 1$ the experimental error in $\exp(-\tau)$ leads to the total uncertainty in temperature. Indeed, we see that the average temperature is defined only for the core of the line where $\tau \approx 1$. The average temperature can also be calculated from the theoretical values of the emission intensity and optical thickness, which is compared with experiment in Fig. 7. Experiment and calculation are in agreement and both show a certain dip in the line center due to the self-absorption.

B. Optical spectrum

Measured and calculated emission spectra of the helium pulse discharge at initial pressure 400 Torr and $I_{\max} = 1000$ A are shown in Fig. 8. The results of measurements are presented by a number of curves corresponding to different discharge runs under the same conditions. They partly overlap and the distinction between them constitutes 10–25 % and shows the accuracy of measurements.

The features in experimental curves at $\lambda = 447$, 606, and 663 nm correspond to forbidden lines. Their parameters are not presented in Ref. [27], so these lines are not taken into account in our calculations.

An agreement between the calculation and experiment on the whole is quite satisfactory. The calculation error is comparable with the measurement error; it is approximately 10% at the ''red'' part of the spectrum considered and ~30% at the ''blue'' one.

VI. CONCLUDING REMARKS

In the experiment presented, continuous spectra of dense helium plasma are measured and studied in detail at electron densities of the order of 10^{18} cm^{-3}. This study completes the set of results for density and correlation effects in the radiation of noble gas plasmas. Many theoretical and experimental studies have been published in the last few decades on the radiative properties of argon, krypton, and xenon dense plasmas (see, e.g., [19,45,46], and references cited therein). For heavy noble gases, electron densities higher than in the present work were achieved (like 10^{19}–10^{20} cm^{-3}), and pronounced coupling effects in continuous absorption have been noticed (relative ''clearing up'' of some parts of the spectra as densities increase [5,14,47]). In contrast, our results show that for electron densities obtained in the experiment the ideal He atom picture still valid for the description of radiation, even though the relations between partially dissolved spectral lines and continuum differ from ideal plasma ones [43].

Calculations of the radiative emission from the flash lamp are made taking into account the influence of plasma microfields on the discrete and continuum spectra. We use a method based on the semiclassical quantum defect theory and take into account the moderately dense effects in the near-threshold spectral region, assuming an unperturbed oscillator strength distribution. For the estimation of the line dissolution the UF approximation is used, while the NN approximation, which is appropriate for heavy noble gas atoms [16,19], seems inadequate for helium. This method leads to the shift and smoothing of the photoionization threshold [19]

and provides the correct behavior of the calculated spectrum in the near-threshold region. Radial profiles of temperature and electron and atomic densities are deduced from the measurements of the transverse distributions of the emission intensity at fixed wavelengths in the spectral range free of lines. The values of temperature and electron density obtained are confirmed by absorption measurements of the He I line at 587.5 nm and He-Ne laser interferometry, respectively. As a result, good agreement between the measured and calculated spectra is obtained for dense He plasmas studied (Fig. 8). Coupling effects manifest themselves at these densities mainly through the statistical character of quasistatic microfield actions on radiators. Some discrepancy between measurements and calculation for the short-wavelength part of the spectra needs further study.

Detailed review of available data on Kr plasmas [47] shows the importance of taking into account the statistical character of plasma microfields as a basis both for proper description of moderately dense plasmas spectra, and for reliable self-consistent diagnostics of such plasmas. For example, the results of direct extrapolation of standard electron temperature diagnostics [43] from the ratios of total spectral line intensities to underlying continuum intensities may become uncertain under redistribution of continuum intensities along the spectrum (as presented in Fig. 3). It concerns both our experimental data for high pressure discharges (preliminary results are given in Ref. [48]) and recent data on discharges in liquid helium [49].

We note that, in contrast with heavy noble gas plasmas, experimental hydrogen plasma spectra were described at electron densities up to 10^{19} cm^{-3} within the framework of the weakly nonideal plasma conception for radiative properties [50] (only for higher densities may some discrepancy be expected [51]). It therefore seems natural that our results obtained for spectral lines and continuous spectra of helium plasma just at densities around 10^{18} cm^{-3} manifest relatively moderate density effects, although the spectra themselves are not simple to interpret. Further experimental study of helium plasmas at higher electron densities ($\sim 10^{19}$ cm^{-3}) generated in capillary discharges [50,51] will be started in the near future to extend our understanding of dense plasma opacity and spectra evolutions as electron density increases.

ACKNOWLEDGMENTS

We would like to thank Professor Ronald McCarroll for discussions and for reading the manuscript. This work was partially supported by NATO Linkage Grant No. HTECH.LG 960803 and Russian Foundation for Basic Research under Grant No. 98-02-18290.

[1] *Strongly Coupled Plasma Physics*, edited by H. M. Van Horn and S. Ichimaru (University of Rochester Press, Rochester, 1993).

[2] *Radiative Properties of Hot Dense Matter. Proceedings of the 4th International Workshop. Sarasota, Florida, 1990*, edited by W. Goldstein, C. Hooper, J. Gaunthier, J. Seely, and R. Lee (World Scientific, Singapore, 1991).

[3] *The Opacity Project*, edited by M. J. Seaton (IOP, Bristol, 1995), Vol. 1.

[4] F. J. Rogers and C. A. Iglesias, in *Strongly Coupled Plasma Physics*, edited by H. M. Van Horn and S. Ichimaru (University of Rochester Press, Rochester, 1993), pp. 243–251.

[5] *Transport and Optical Properties of Nonideal Plasma*, edited by G. A. Kobzev, I. T. Iakubov, and M. M. Popovich (Plenum, New York, 1995).

[6] Yu. K. Kurilenkov and H. M. Van Horn, in *The Equation of States in Astrophysics, Proceedings of the International Astronomical Union (IAU) Colloquium No. 147*, Saint-Malo, France, 1993 (Cambridge University Press, Cambridge, 1994), pp. 581–585.

[7] J. R. Roberts and X. Voigt, J. Res. Natl. Bur. Stand., Sect. A **75A**, 291 (1971).

[8] V. Ruzdjak and V. Vujnovic, Astron. Astrophys. **54**, 751 (1977).

[9] A. Unsöld, Z. Astrophys. **24**, 355 (1948).

[10] I. V. Avilova and G. E. Norman, Teplofiz. Vys. Temp. **2**, 517 (1964).

[11] H. Gündel, Beitr. Plasmaphys. **11**, 1 (1971).

[12] G. A. Kobzev, Zh. Eksp. Teor. Fiz. **61**, 582 (1971) [Sov. Phys. JETP **34**, 310 (1971)].

[13] V. Ts. Gurovich and V. S. Engelsht, Zh. Eksp. Teor. Fiz. **72**, 445 (1977) [Sov. Phys. JETP **45**, 232 (1977)].

[14] G. A. Kobzev, Yu. K. Kurilenkov, and G. E. Norman, High Temp. **15**, 163 (1997); G. A. Kobzev and Yu. K. Kurilenkov, *ibid.* **16**, 385 (1978).

[15] V. Sevastyanenko, Contrib. Plasma Phys. **25**, 151 (1985).

[16] V. E. Gavrilov and T. V. Gavrilova, Opt. Spektrosk. **63**, 727 (1987) [Opt. Spectrosc. **63**, 429 (1987)].

[17] D. G. Hummer and D. Mihalas, Astrophys. J. **331**, 794 (1988).

[18] E. J. Iglesias and H. R. Griem, J. Quant. Spectrosc. Radiat. Transf. **55**, 383 (1996).

[19] L. G. D'yachkov, Y. K. Kurilenkov, and Y. Vitel, J. Quant. Spectrosc. Radiat. Transf. **59**, 53 (1998).

[20] D. J. Heading, J. P. Marangos, and D. D. Burgess, J. Phys. B **25**, 4745 (1992).

[21] S. Büscher, S. Glenzer, Th. Wrubel, and H.-J. Kunze, J. Quant. Spectrosc. Radiat. Transf. **54**, 73 (1995).

[22] H. Suemitsu, K. Iwaki, Y. Takemoto, and E. Yoshida, J. Phys. B **23**, 1129 (1990).

[23] K. Günther, M. M. Popovich, S. S. Popovich, and R. Radtke, J. Phys. D **9**, 1139 (1976).

[24] K. Günther, S. Lang, and R. Radtke, J. Phys. D **16**, 1235 (1983).

[25] Y. Vitel, M. Skowronek, K. Benisty, and M. M. Popovic, J. Phys. D **12**, 1125 (1979).

[26] Y. Vitel and M. Skowronek, in *Proceedings of the 8th European Sectional Conference on Atomic and Molecular Physics on Ionized Gases*, edited by A. Bethke (Greifswald University Press, Greifswald, GDR, 1986), pp. 297–298, 299–300.

[27] H. Griem, *Spectral Line Broadening by Plasmas* (Academic, New York, 1974).

[28] C. F. Hooper, Jr., Phys. Rev. **165**, 215 (1968).

[29] L. G. D'yachkov, J. Quant. Spectrosc. Radiat. Transf. **59**, 65 (1998).
[30] M. J. Seaton, J. Phys. B **23**, 3255 (1990).
[31] L. G. D'yachkov and P. M. Pankratov, J. Phys. B **24**, 2267 (1991).
[32] L. G. D'yachkov and P. M. Pankratov, J. Phys. B **27**, 461 (1994).
[33] L. G. D'yachkov, Opt. Spektrosk. **81**, 885 (1996) [Opt. Spectrosc. **81**, 809 (1996)].
[34] U. Fano and J. Cooper, Rev. Mod. Phys. **40**, 441 (1968).
[35] L. M. Biberman and G. E. Norman, Usp. Fiz. Nauk **91**, 193 (1967) [Sov. Phys. Usp. **10**, 52 (1967)].
[36] L. G. D'yachkov, Opt. Spektrosk. **61**, 688 (1986) [Opt. Spectrosc. **61**, 608 (1986)].
[37] D. Hofsaess, J. Quant. Spectrosc. Radiat. Transf. **19**, 339 (1978).
[38] L. D. Landau and E. M. Lifshitz, *Statistical Physics* (Pergamon, London, 1958).
[39] H. Bartels, Z. Phys. **136**, 411 (1953).
[40] H. Zwicker, in *Plasma Diagnostics*, edited by W. Lochte-Holtgreven (North-Holland, Amsterdam, 1968), p. 214.
[41] D. E. T. F. Ashby and D. F. Jephcott, Appl. Phys. Lett. **3**, 13 (1963).
[42] D. E. T. F. Ashby, D. F. Jephcott, A. Malein, and F. A. Rayner, Appl. Phys. Lett. **36**, 29 (1965).
[43] H. R. Griem, *Plasma Spectroscopy* (McGraw-Hill, New York, 1964).
[44] H. W. Drawin, Z. Phys. **228**, 99 (1969).
[45] V. E. Gavrilov, T. V. Gavrilova, and V. E. Fortov, High Temp. **28**, 453 (1990).
[46] A. T. M. Wilbers, G. M. W. Kroesen, C. J. Timmermans, and D. C. Schram, J. Quant. Spectrosc. Radiat. Transf. **45**, 1 (1991).
[47] Y. Vitel, L. G. D'yachkov, and Yu. K. Kurilenkov, J. Phys. B **30**, 2021 (1997).
[48] Y. Vitel, M. El Bezzari, L. G. D'yachkov, and Yu. K. Kurilenkov, in *XXIII International Conference on Phenomena in Ionized Gases, Proceedings, Contributed Papers*, edited by M. C. Bordage and A. Gleizes (Université Paul Sabatier, Toulouse, France, 1997), Vol. I, pp. 190 and 191.
[49] W. Qin, K. Minami, A. W. De Silva, and F. Tomimoto, in *XXIII International Conference on Phenomena in Ionized Gases, Proceedings, Invited Papers*, edited by M. C. Bordage and A. Gleizes [J. Phys. IV **7**, C4-319 (1997)].
[50] T. V. Gavrilova, V. P. Averyanov, Y. Vitel, L. G. D'yachkov, and Yu. K. Kurilenkov, Opt. Spektrosk. **82**, 757 (1997) [Opt. Spectrosc. **82**, 701 (1997)].
[51] T. V. Gavrilova, V. P. Averyanov, Y. Vitel, C. Le Guen, L. G. D'yachkov, and Yu. K. Kurilenkov, in *XXIII International Conference on Phenomena in Ionized Gases, Proceedings, Contributed Papers*, edited by M. C. Bordage and A. Gleizes (Université Paul Sabatier, Toulouse, France, 1997), Vol. I, pp. 188 and 189.